Technological University Dublin
ARROW@TU Dublin

Articles | Centre for Industrial and Engineering Optics

2010-01-01

Optical Properties of Photopolymer Layers Doped with Aluminophosphate Nanocrystals

Elsa Leite
Technological University Dublin

Tzvetanka Babeva
Bulgarian Academy of Sciences

E Ng
Laboratoire Catalyse & Spectrochimie (LCS), ENSICAEN - Université de Caen

See next page for additional authors

Follow this and additional works at: https://arrow.tudublin.ie/cieoart

 Part of the Condensed Matter Physics Commons, and the Optics Commons

Recommended Citation

Leite, E. et al. (2010) Optical Properties of Photopolymer Layers Doped with Aluminophosphate Nanocrystals. *Journal of Physical Chemistry C*. doi:10.1021/jp1060073

This Article is brought to you for free and open access by the Centre for Industrial and Engineering Optics at ARROW@TU Dublin. It has been accepted for inclusion in Articles by an authorized administrator of ARROW@TU Dublin. For more information, please contact arrow.admin@tudublin.ie, aisling.coyne@tudublin.ie, vera.kilshaw@tudublin.ie.

Authors
Elsa Leite, Tzvetanka Babeva, E Ng, Vincent Toal, Svetlana MIntova, and Izabela Naydenova

This article is available at ARROW@TU Dublin: https://arrow.tudublin.ie/cieoart/35

Optical Properties of Photopolymer Layers Doped with Aluminophosphate Nanocrystals

E. Leite,[a] Tz. Babeva,[b] E.-P. Ng,[c,d] V. Toal,[a] S. Mintova,[c,*] I. Naydenova[a,*]

[a]*Centre for Industrial and Engineering Optics, School of Physics, Dublin Institute of Technology, Kevin Street, Dublin 8, Ireland*
[b]*Central Laboratory of Photoprocesses, Bulgarian Academy of Sciences, Acad. G. Bonchev Str., Bl. 109, 1113 Sofia, Bulgaria*
[c]*Laboratoire Catalyse & Spectrochimie (LCS), ENSICAEN - Université de Caen – CNRS, 6, boulevard du Maréchal Juin, 14050 Caen Cedex, France*
[d]*Current address: School of Chemical Sciences, Universiti Sains Malaysia, 11800 USM, Pulau Pinang, Malaysia*

The optical properties of photopolymer layers consisting of an acrylamide–based matrix and microporous aluminophosphate nanocrystals of AEI- type are investigated. The compatibility of the photopolymer doped with the nanoparticles is studied. The surface and volume properties of the layers with different levels of doping with microporous nanocrystals are characterized. The effective refractive indices and absorption coefficients of the doped photopolymer layers are determined and used to calculate the refractive index and porosity of pure AEI nanoparticles used as dopants. Volume transmission gratings were recorded in the doped photopolymer layers at different spatial frequencies. By spatial monitoring of the characteristic Raman peak of the AEI particles across the grating vector, the optimal concentrations of the nanocrystals for obtaining highest light induced redistribution of nanocrystals are determined. The optical properties of the photopolymer layers combined with the redistribution of the AEI nanoparticles during holographic recording are the parameters exploited for fabrication of optical sensors. An irreversible humidity sensor based on a transmission holographic grating is designed and fabricated. The diffraction efficiency of the sensor changes permanently after exposure to high humidity.

Keywords: holography, photopolymer, nanoparticles, optical properties, porosity, humidity indicator.

Introduction

Holographic dry photopolymers have received much attention due to their possible applications in diffractive optics, information storage and displays, and sensors.[1-6] Special attention is paid to the optical properties of hybrid organic/inorganic materials which have been used in non-conventional applications such as photovoltaic cells and light-emitting devices, and biosensors.[7-11]

The development of these hybrid organic/inorganic materials was inspired by the phenomenon of light induced mass transport in photopolymerizable materials, which leads to improved holographic properties. The basic idea behind the concept of the photopolymerizable nanocomposites is to introduce nano-dopants with significantly different refractive index from that of the host material and to achieve redistribution of the nano- dopants during holographic recording.[12-17] It has been shown that optimum values of recording intensity and volume fractions of incorporated solid nanoparticles such as SiO_2[18], TiO_2[19] and ZrO_2[20], lead to an increase of diffraction efficiency of the recorded gratings due to a higher refractive index modulation. However, the process of dispersing variable types of nanoparticles in a polymer matrix is problematic since poor compatibility between the polymer host and the dopants is observed. Besides, the nano- dopants produce optical losses due to increased scattering caused by the nanoparticles, and the large difference between their refractive index and that of the photopolymer matrix.

In addition to metal oxide nanoparticles, the use of colloidal zeolites (microporous crystalline materials with size less than 300 nm, uniform pore size and ordered structure) in photopolymer-water solution yielding good optical quality of the dry layers has been reported.[21-23] The refractive index of the zeolite particles is close to that of the photopolymer, and the optical losses are quite low even in the case of relatively big nanoparticles (diameter of 100-300 nm).[23-25] Additional advantages of using zeolites as dopants are related to the possibility to control their chemical composition, pore shapes and sizes, hydrophilicity, hydrophobicity and overall particle size and morphology.[26]

Understanding and predicting the influence of porosity and optical properties of microporous nanoparticles on the effective optical properties of the photopolymer layers will be beneficial for

their applications, in particular in holographic sensor design. Moreover, it will be possible to characterize the optical properties of the microporous nanomaterials incorporated in the photopolymer layers taking into consideration the strong influence of fill/empty effects of the pores.

The aim of this work is to study the optical properties of photopolymer layers consisting of an acrylamide–based matrix and microporous aluminophosphate nanocrystals (AlPO-18, AEI- type framework structure).[27] Besides, an irreversible humidity indicator based on a transmission holographic grating in the photopolymer layers doped with the AlPO-18 nanoparticles is demonstrated. A detailed characterization and optimization of the sensor is in progress and will be published elsewhere.

Theory

A simple transmission volume phase hologram can be recorded when the photosensitive medium is located in the area of overlap of two coherent beams of light of appropriate wavelength (Figure 1A). The spatial frequency of the transmission hologram is determined by the angle between the two recording beams and it is given by:

$$2\Lambda \sin\theta = \lambda , \qquad (1),$$

where Λ is the fringe spacing, θ is half of the angle between the two recording beams and λ is the wavelength of the recording beams.

It has been previously shown[12-22] that the holographic recording process in nanoparticle doped photopolymerisable materials can lead to the redistribution of the nanoparticles and thus to the creation of patterns of particle rich and particle depleted areas (Figure 1B).

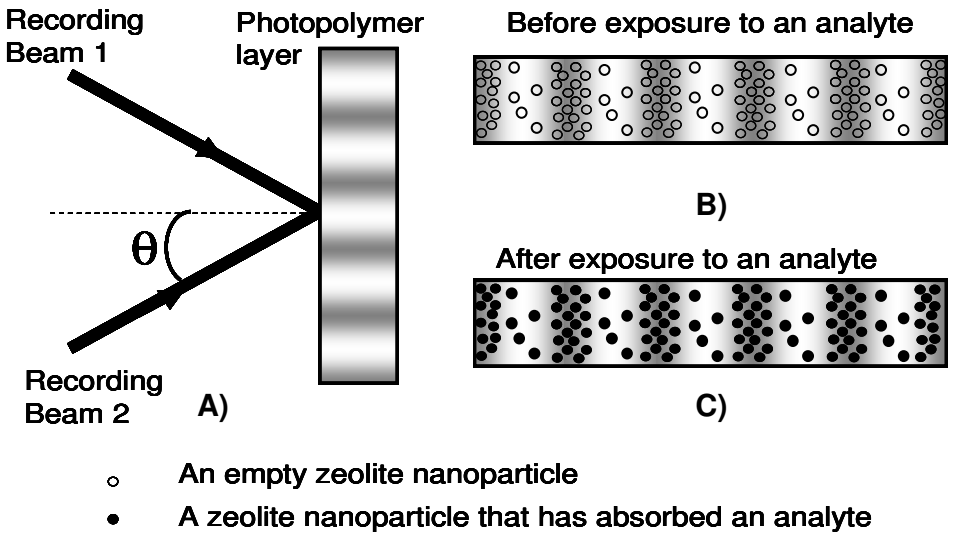

Figure 1. A) Recording of a transmission hologram, B) the spatial redistribution of microporous nanoparticles as a result of holographic recording and C) after exposure to an analyte.

The diffraction efficiency, η, of such a volume phase hologram is given by (2):[28]

$$\eta = \sin^2\left(\frac{\pi n_1 d}{\lambda \cos\theta}\right), \qquad (2),$$

where n_1 – is the refractive index modulation (the difference between the refractive indices in illuminated and non illuminated areas), d is the thickness of the hologram, λ is the wavelength of the probe beam that is used to measure the diffraction efficiency, θ is the Bragg angle.

The modulation of the optical refractive index n_1 is caused by: 1) polymerisation of the monomer and its conversion into polymer; 2) density variation due to concentration driven monomer diffusion from dark to bright fringe areas; 3) density variation due to concentration driven diffusion of short polymer chains from bright to dark fringe areas; 4) spatial patterning of the nanozeolite particles characterised by significantly different refractive index from that of the photopolymer matrix.

The contribution made by the redistributed nanoparticles to the overall refractive index modulation can be estimated by:[29]

$$\Delta n = \frac{2 f_{nanodopants}}{\pi} (n_{nanodopant} - n_{host}) sin(\alpha\pi) \quad (3),$$

where $f_{nanodopants}$ is the volume fraction of nanoparticles in the nanoparticle-rich region, $n_{nanodopant}$ is the refractive index of the nanodopants, n_{host} is the refractive index of the host organic matrix, and α is the fraction of the period with a rich content of nanoparticles. By measuring the diffraction efficiency and determining the refractive index modulation amplitude in doped and undoped layers one can estimate the volume fraction of redistributed nanoparticles, $f_{nanodopants}$.

In order to achieve maximum benefit to the refractive index modulation during holographic recording from the presence of the nanoparticles in the layer it is necessary to maxmize redistribution of the nanoparticles. Choosing maximum difference between the refractive index of the nanoparticles and that of the host photopolymer matrix will also increase their positive effect on the final refractive index modulation. At the same time, a careful consideration must be given to the increased optical scattering due to the large difference in the refractive indices. Thus in determining what the optimum concentration of the nanoparticles is being a balance should be sought between the optical losses and the improved refractive index modulation.

The basic concept behind the design of holograms recorded in microporous nanoparticles doped photopolymer layers for application in sensing is that adsorption/absorption of the specific analyte will cause the refractive index of the nanoparticles to change. When they are redistributed this will lead to a change in the total refractive index modulation and thus the analyte's presence will be observed as a change of the diffraction efficiency of the hologram.

Experimental Section

A) Preparation of microporous AlPO-18 nanocrystals

AlPO-18 nanocrystals were prepared according to the following procedure: 31.04 g of Aluminum isopropoxide (Aldrich, 98%) was dissolved in 202.08 g of tetraethylammonium hydroxide (TEAOH, Aldrich, 35%) and 114.76 g distilled water, followed by vigorous stirring until a clear solution was obtained. Then 55.36 g of phosphoric acid (Acros, 85%) was added drop wise under continuous stirring. The resulting mixture was stirred for 45 minutes in order to ensure a water-clear suspension. The final composition of the suspension was 1 Al_2O_3 : 3.16 P_2O_5 : 3.16 $(TEA)_2O$: 186 H_2O. Crystallization of AlPO-18 nanocrystals from this suspension was

carried out at 180 °C in a microwave oven for 5 min (Sample 1) and in a conventional oven for 18 h (Sample 2). After the syntheses, the crystalline suspensions were purified using high-speed centrifugation (24,500 rpm for 10 min) in three consecutive steps and re-dispersed in water using an ultrasonic bath. The AlPO-18 nanocrystals were finally stored in water with a solid concentration of 6 wt. % and pH of 7.

Preparation of photopolymer layers doped with AlPO-18 nanocrystals. The photopolymer layers consisting of a soft photopolymer matrix and AlPO-18 nanoparticles were prepared according to the procedure described below. A photopolymer solution developed at the Centre for Industrial and Engineering Optics-Dublin Institute of Technology is used as a matrix.[30] It consists of 9 ml stock solution of polyvinyl alcohol (PVA, 20 w/w %), 2 ml triethanolamine, 0.6 g acrylamide, 0.2 g N,N-methylene bisacrylamide, and 4 ml Erythrosin B dye of 1.1 mM dye stock solution.

The aqueous suspensions of AlPO-18 nanoparticles were sonicated for 20 minutes prior mixing with the photopolymer solution in order to ensure disintegration of any possible agglomerates. The AlPO-18 nanocrystals in water suspension were added to the photopolymer with the following concentrations 0, 2.5, 5, and 10 wt. %. Detailed information on the mixing procedure can be found elsewhere.[22,23] The photopolymer/ AlPO-18 suspension (0.5 ml) was deposited on glass plates (26 x 38 mm^2) followed by drying for 24 h in a dark room at ambient conditions ($T = 21 \pm 3\ ^{o}C$ and relative humidity, RH = 40 - 60 %) on an optical table.

B) Characterization of the nanocomposite layers

Volume characterisation of suspensions and layers. Dynamic light scattering (DLS) measurements using a Malvern Zetasizer Nano ZS were carried out on pure AlPO-18 suspensions and on photopolymer doped with AlPO-18 nanocrystals to determine the mean diameter of the nanoparticles and to monitor their stability. DLS measurements of the suspensions were performed immediately after mixing the photopolymer with the AlPO-18 suspension, and again, after 24 hours in order to check their stability with time. Additionally, the surface charge and degree of agglomeration of the AlPO-18 nanoparticles were determined by measuring the zeta potential value at a constant concentration (6 wt. %) and pH=7.

The morphology and size of the nanocrystals were studied by scanning electron microscopy (SEM) using a Philips XL 30 microscope. The crystallinity of the freeze-dried AlPO-18 powder

was proven by X-ray diffraction (XRD) analysis carried out with a STOE STADI-P X-ray diffractometer. The porosity of the AlPO-18 powder was determined by measuring the nitrogen sorption isotherms of calcinated sample (390 °C for 12 h) with a Micromeritics ASAP 2010 surface area analyzer.

Transmittance (T, accuracy 0.1 %) and reflectance (R, 0.5 %) spectra of the photopolymer layers doped with AlPO-18 nanoparticles were recorded using a high precision UV-VIS-NIR spectrophotometer, CARY 5E VARIAN.

The Raman measurements on the photopolymer layers doped with AlPO-18 nanocrystals were performed using a Horiba Jobin Yvon confocal Raman spectrometer with a confocal pinhole diameter of 100 μm and an excitation line of 532 nm (the magnification of the microscope objective was 100X). The confocal Raman spectroscopy was used to study the distribution of the particles through the thickness of the photopolymer layers.

Characterization of layers' surface. The photopolymer layers doped with different concentrations of AlPO-18 nanocrystals were exposed simultaneously to UV and visible light (LV202 Megaelectronics) with an intensity of 2.5 mW/cm^2 for 30 min to achieve complete photopolymerisation.

The surfaces of the layers were studied using a White Light Interferometric (WLI) surface profiler, MicroXAM S/N 8038, with vertical and lateral resolution of 1 nm and 1 μm, respectively.

Confocal Raman spectroscopy was used to study the particle distribution in direction parallel to the wave vector of recorded transmission grating.

Holographic recording in photopolymer layers doped with AlPO-18 nanocrystals. Holographic transmission gratings of spatial frequency of 500 and 2000 $l \cdot mm^{-1}$ were recorded by exposure of the layers to two mutually coherent s-polarized beams of wavelength 532 nm, and total exposure energy of 600 $mJcm^{-2}$. The grating growth was monitored in real time by probing it with an unexpanded He-Ne laser beam of wavelength 633 nm incident at the Bragg angle. The sample was held on a rotation stage, allowing the angular selectivity of the grating to be measured, following recording, by varying the incident angle of the probe beam. The angular selectivity curve was used to determine the effective thickness of the grating. This parameter and the maximum diffraction efficiency, η (here defined by the ratio of the intensity of the first

diffraction order and the incident intensity of the probe beam) were used to calculate the refractive index modulation amplitude, n_1, using Kogelnik's coupled wave theory:[28]:

$$n_1 = \frac{\lambda \cos(\theta) \arcsin(\sqrt{\eta})}{\pi d} \quad (4),$$

where λ and θ are the reconstructing beam wavelength and incident angle, respectively and d is the thickness of the photosensitive layer.

Testing of volume transmission gratings of layers for humidity sensing. A controlled environment chamber with an Electro-Tech Systems model 503-20 humidity system was used to characterize the volume transmission holograms. The initial diffraction efficiency was measured when the layers were exposed to 15 % relative humidity (RH). Then the layers were placed in an oven at 120 ^{o}C for 15 minutes to expel the water from inside the pores of the AlPO-18 nanocrystals. The layers were then immediately placed inside the humidity chamber, where RH was raised to 60 %, and the diffraction efficiency was monitored until no further change was observed. Finally, the RH was returned to 15 % and the change in diffraction efficiency was monitored over time.

Results and Discussion

Volume characterization of suspensions and layers. The particle size distribution (PSD) of the AlPO-18 nanocrystals as-prepared and after storing at ambient conditions for one month, was investigated by DLS. The average size of crystals was about 190 - 210 nm for both samples (see Figure 2A). The initial and final data points for both DLS curves were almost the same. Thus, it could be concluded that the AlPO-18 nanocrystals synthesized under microwave and conventional heating have similar crystal sizes. The widths of the PSD curves were similar thus proving the relative stability of the particles at a given concentration in water dispersant. In addition, the stability of the AlPO-18 nanoparticles in the water suspension (solid concentration of 6 wt. % and pH = 7) was determined by zeta potential measurements. The zeta potential value for the AlPO-18 nanocrystals in the water is above -40 mV, which explains their long-term

stability in the colloidal form (Table 1).[31] No sedimentation in the crystalline suspensions was observed after a month at ambient conditions.

The crystalline nature of the microporous AlPO-18 nanoparticles was proven by the XRD patterns shown in Figure 2B. The XRD patterns exhibit the typical Bragg reflections for AEI-type crystalline structure. The intensity and line widths of the peaks are identical for both the as prepared and calcined (see experimental section) samples, thus revealing that the AlPO-18 nanocrystals do not change their crystallinity and size during the post-synthesis treatment. No difference was observed between the XRD patterns of samples 1 and 2 thus confirming their high degree of crystallinity.

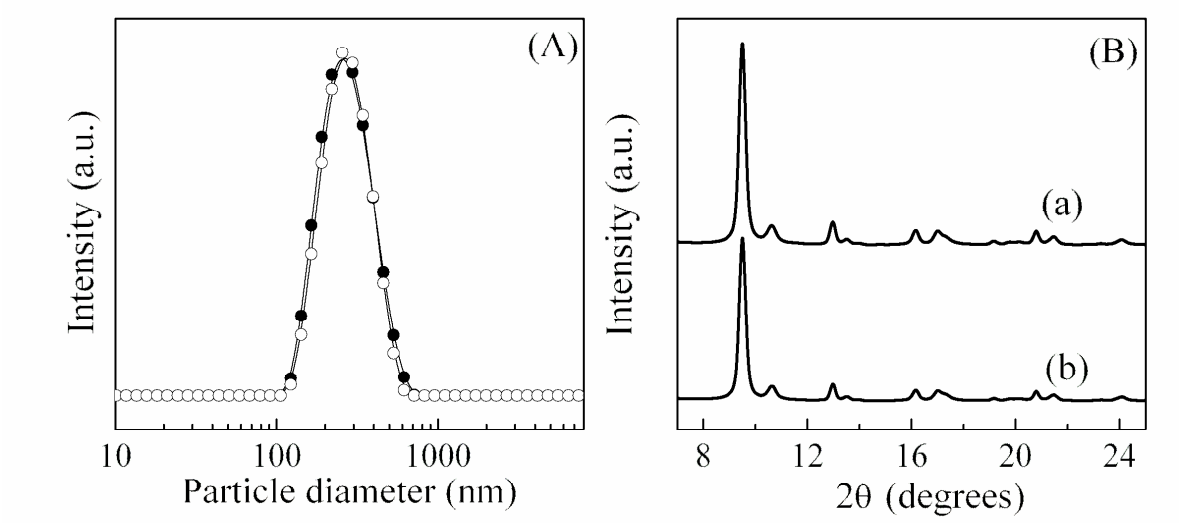

Figure 2. (A) Dynamic Light Scattering curves of AlPO-18 nanocrystals from sample 1 (full circle) and sample 2 (open circle). (B) X-ray diffraction patterns of AlPO-18 nanocrystals from sample 1 (a) as-prepared and (b) calcined (390 °C for 12 h). The XRD patterns of sample 2 are identical and not shown here.

The morphological features of the AlPO-18 nanoparticles were examined by scanning electron microscopy. All AlPO-18 nanocrystals have elongated elliptical shape, which is different from the micron sized crystals with typical tetragonal shape (Figure 3). As can be seen, the synthesis of AlPO-18 from highly supersaturated suspensions with excess of organic template (TEAOH) in both microwave and conventional ovens results in the formation of highly stable and homogeneous nanoparticles. The size of the AlPO-18 nanocrystals determined from the SEM pictures is approximately that obtained from the DLS data, i.e. ranging from 180 to 220 nm. The particle sizes of AlPO-18 were also evaluated by measuring the dimensions of numerous crystals in three directions on the SEM pictures. Nanocrystals have flat elliptical shape with major and minor diameters of (237 ± 26) nm and (172 ± 35) nm, respectively. The thickness of the crystals estimated from the SEM picture shown in Figure 3b is about 30 nm

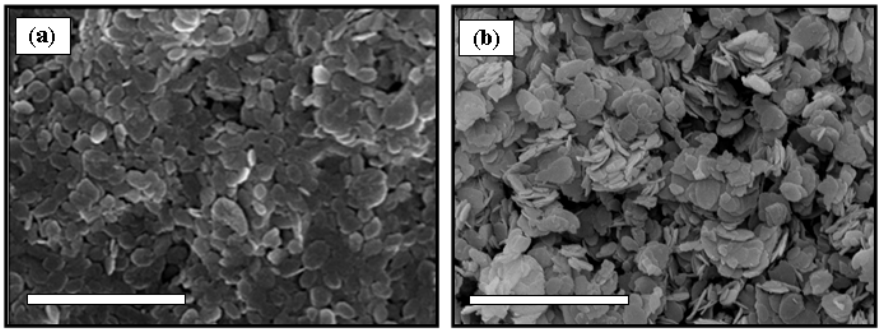

Figure 3. SEM images of AlPO-18 nanocrystals from (a) sample 1 and (b) sample 2.

Scale bar, M = 2 μm.

The general characteristics of the AlPO-18 nanocrystals are summarized in Table 1. As expected the Al/P ratio is almost 1, so that an “electrically” neutral framework structure is formed.

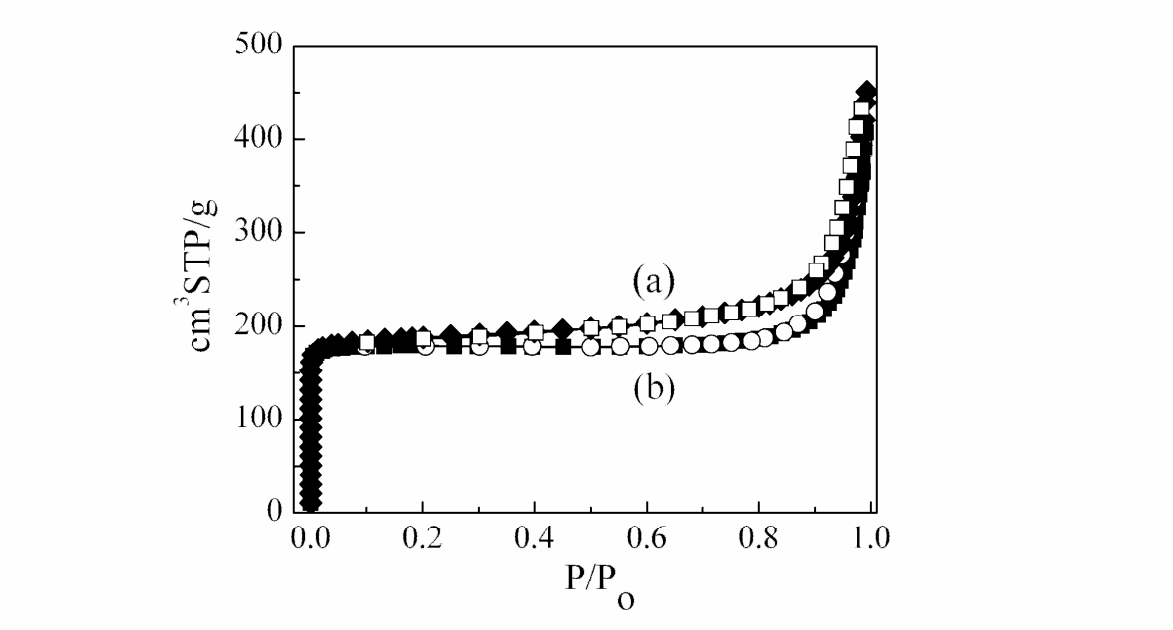

Figure 4. Nitrogen adsorption/desorption isotherms of AlPO-18 nanocrystals from (a) sample 1 and (b) sample 2.

The porosity of the AlPO-18 nanocrystals from samples 1 and 2 has been determined by N_2 sorption measurements (Figure 4). The nitrogen adsorption-desorption curves show the typical type IV isotherm with a type H1-H3 hybrid loop in accordance with IUPAC classification (Figure 4).[32] Both isotherms exhibit a rapid increase in nitrogen uptake at low relative pressure ($P/P_o < 0.1$), which corresponds to the filling of the micropores (3.8 Å size of) with nitrogen. A plateau with an abrupt inclination step at high relative pressure ($P/P_o > 0.8$) was observed, which is associated with multilayer adsorption in the textural mesopores of the nanosized material. Both samples have the same initial N_2 uptake, thus suggesting a similar micropore volume (0.21 cm^3/g) and crystal size (190 nm) (see Table 1). The total specific pore volume is 0.70 cm^3/g, which is due to the small crystal size of the nanoparticles. Both samples have high surface area (> 500 cm^2/g), which can be explained by their high degree of crystallinity.

AlPO-18 suspensions (samples 1 or 2) in photopolymer with concentrations of 2.5, 5, and 10 wt. % were compared with the pure photopolymer. The compatibility of the AlPO-18 nanocrystals with the photopolymer solutions was measured by collecting the DLS curves of the as-prepared mixtures and after 24 h aging at ambient conditions. It is observed that the size of the

particles does not change, and the PSD curves have the same maximum. No aggregation of the AlPO-18 nanoparticles is observed even after 24 h.

The solutions of photopolymer doped with the AlPO-18 nanocrystals (0, 2.5, 5, and 10 wt. %) were deposited on high refractive index glass substrates and after drying at ambient conditions were subjected to volume optical characterization. Primarily, the volume characterization of the layers was performed by Raman spectroscopy. The nominal depth resolution of the Raman spectrometer is determined by the focal depth of the focused laser beam, which is influenced by the refraction of laser beam at air/layer interface. The depth resolution in our case was determined by measuring the intensity of the Raman peak due to the Si band at 522 cm^{-1} while an Si surface was translated through the focus point along the beam propagation axis (direction normal to the surface).[33] Figure 5 presents the intensity of the Si peak at 522 cm^{-1} as a function of the distance from the silicon surface for two samples, i.e. pure Si-surface and Si-surface covered with a photopolymer layer with a thickness of 70 μm. Thus for the first case the negative and positive distance values on x-axis correspond to the distance from the Si-surface in air and in silicon, respectively. When Si surface was covered with the photopolymer layer, the negative and positive values of x-axis correspond to the depth in the photopolymer layer and in the silicon wafer, respectively. It is seen that the Raman signal drops off quickly when the Si surface is out of focus. From the full-width-half-maximum (HWHM) of the curves shown in Figure 5, the nominal depth resolution was determined. The depth resolution measured in air is 3 μm and in the photopolymer is 8 μm.

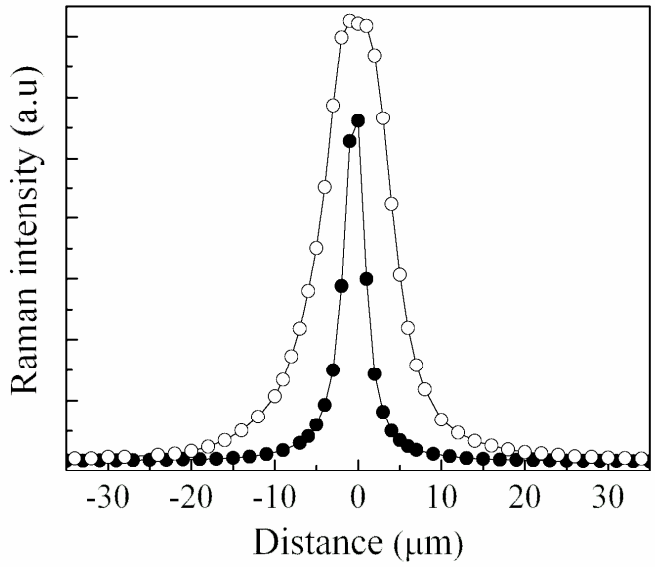

Figure 5. Raman intensity of Si peak at 522 cm^{-1} for a pure silicon surface (filled circles) and a silicon surface covered with a photopolymer layer with a thickness of 70 μm (open circles) as a function of the distance from the Si-interface for a confocal pinhole with a diameter of 100 μm.

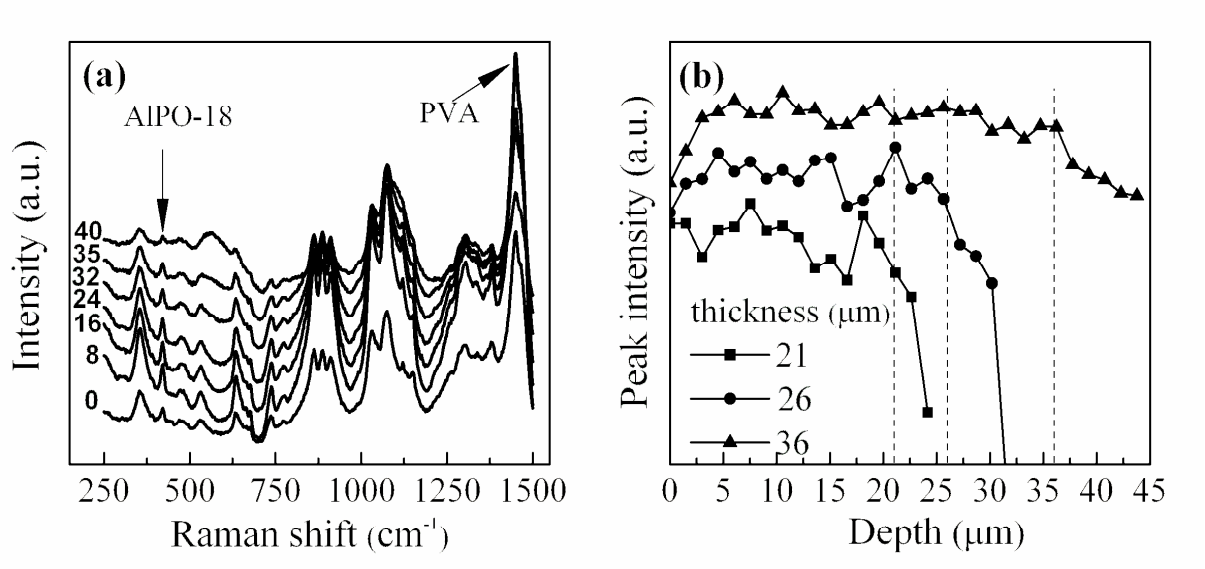

Figure 6. A) Raman spectra of photopolymer layer (thickness 36 μm), doped with 10 wt. % AlPO-18) collected at different penetration depths indicated next to each curve in microns ('0' is the film's surface). The peaks at 421 cm^{-1} and 1450 cm^{-1} are assigned to AlPO-18 nanocrystals and PVA, respectively. B) Distribution of AlPO-18 nanocrystals versus depth. The vertical lines indicate the thickness values measured by WLI profilometry.

The Raman spectra of the photopolymer layers doped with AlPO-18 nanocrystals were collected by focusing the laser beam inside the sample at different distances from the surface in steps of 1.5 μm (Figure 6A). Since the PVA concentration was constant throughout the layer thickness, the spectra were normalized with respect to the PVA peak at 1450 cm^{-1}. Then the intensity of the characteristic peak of AlPO-18 at 421 cm^{-1} was plotted against depth in the layer (Figure 6B). The depth in the layer was calculated as the distance from the surface multiplied by the refractive index of the layer (n = 1.5). As can be seen, there is a very good agreement between the calculated penetration depth and the measured thickness of the layers (see Figure 6). From the Raman depth measurements one can conclude that the AlPO-18 nanocrystals are homogenously distributed throughout the thickness of the layers. If one assumes that the intensity of the signal at 421cm^{-1} is directly proportional to the concentration of the AlPO-18 nanoparticles, then the standard deviation of the concentration throughout the layer can be calculated The standard deviations of particles concentrations from the average value of 10 wt. % across the layers with thicknesses of 21, 26 and 36 μm are 0.6, 0.5 and 0.4 wt. % respectively. This data shows that the AlPO-18 nanoparticles are homogeneously distributed across the layers independently of their thickness, which can be explained by the high compatibility and stability of the photopolymer solutions doped with the microporous nanoparticles.

The volume refractive indices of the photopolymer layers with and without AlPO-18 nanoparticles were determined by measuring the transmittance and reflectance spectra using a high precision UV-VIS-NIR spectrophotometer (Figure 7). The simultaneous determination of the refractive index (n) and the extinction coefficient (k) of the layers was performed by minimization of the goal function consisting of discrepancies between the measured and calculated spectra by a Nelder-Mead simplex method for each wavelength λ in the spectral range 400-800 nm.[23,34] Figure 7 represents the dispersion curves of refractive index of photopolymer

layers doped with AlPO-18 nanocrystals with concentrations of 5 and 10 wt.% in comparison with undoped layers. As can be seen from the Figure 7, the increase of AlPO-18 concentration in the layers results in a decrease in refractive index. The refractive indices of the layers doped with 0, 5 and 10 wt. % AlPO-18 nanocrystals at 532 nm are 1.506, 1.490 and 1.476 (± 0.005), respectively. Considering that the refractive index of AlPO-18 particles is lower than for the photopolymer, a decrease in *n* of the doped photopolymer layers can be expected (see Figure 7).

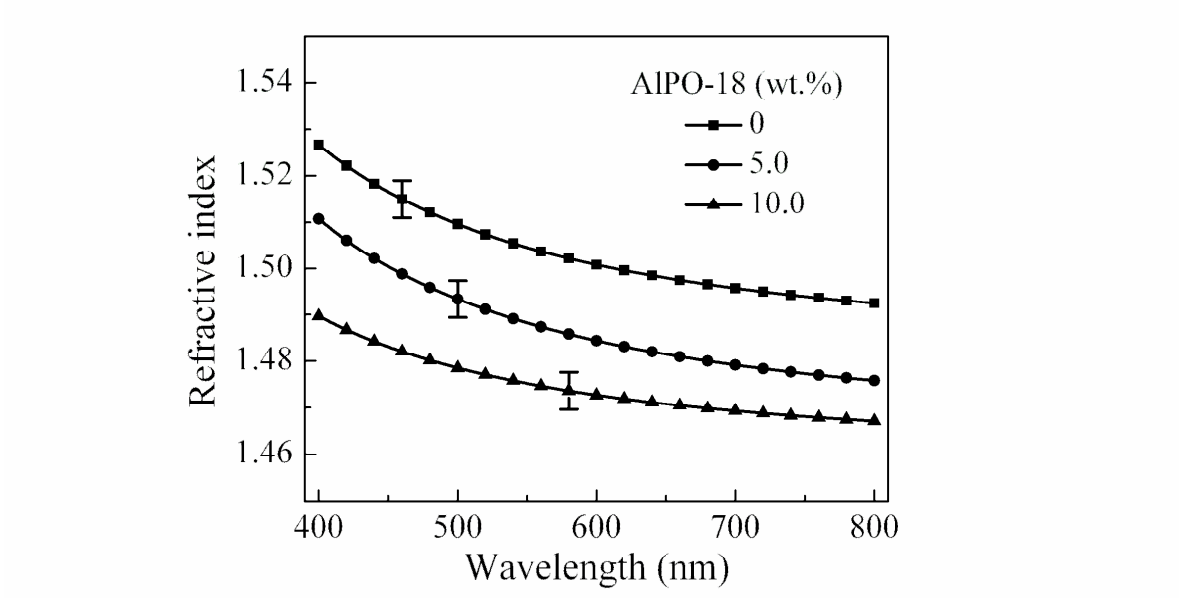

Figure 7. Dispersion curves of refractive index for photopolymer layers doped with AlPO-18 nanocrystals. Error: ±0.005

As shown above, the bulk properties of the layers depend on the interactions between the two components, i.e. the photopolymer and microporous AlPO-18 nanocrystals. Therefore, the possibility of filling the micropores of the AlPO-18 (3.8 Å) with guest molecules was investigated. The porosity of the AlPO-18 nanoparticles incorporated in the photopolymer layers was calculated according to the methods described [23] and compared with the experimental N_2-sorption data (see Table 1). In order to determine the porosity of the nanoparticles, the refractive index of the AlPO-18 is required. For calculation of the refractive index of microporous materials

the Bruggeman effective media approximation (EMA) is used. The idea of EMA is to regard the nanocomposite as a medium with effective refractive index that depends on the refractive index and volume fractions of the two phases presented, i.e. the photopolymer matrix and aluminophosphate nanoparticles. Since the refractive indices of the undoped photopolymer (i.e the matrix) and doped photopolymer (i.e the nanocomposite) are already determined (Figure 7) we are able to calculate the refractive index and volume fraction of the dopant using the recently developed optical method [23]. The dispersion curve for AlPO-18 calculated by this method is presented in Figure 8. For comparison the dispersion curves for pure Al_2O_3 and P_2O_5 are given as well.[35,36] The effective refractive index of a mixture from Al_2O_3 and P_2O_5 in the ratio 1 : 1 is included also because the Al/P ratio in the AlPO-18 nanocrystals is about 1 as determined by X-ray fluorescence chemical analyses (Table 1). The refractive index and density of the mixture (Al_2O_3 : P_2O_5) was calculated by Bruggeman EMA using the refractive indices of Al_2O_3 and P_2O_5, and volume fractions calculated using oxide densities values of 4 g/cm^3 [37] and 2.4 g/cm^3 [37] for Al_2O_3 and P_2O_5, respectively. Further if one assumes that the AlPO-18 nanocrystals consist of two phases – air and mixture Al_2O_3 : P_2O_5 one can calculate the volume fraction of the two phases using the Bruggeman effective media approximation. Using this approach, it was determined that the AlPO-18 nanoparticles consist of 71 % oxides (Al_2O_3 : P_2O_5) mixture and 29 % voids. Based on the density values of Al_2O_3 and P_2O_5 and their volume fractions, the density of a mixture of Al_2O_3 : P_2O_5 is estimated. Considering both that the calculated density of mixture is 3 g/cm^3 and the free volume of AlPO-18 is 29 % from the total volume of the nanoparticle fraction, the density of AlPO-18 particles was determined to be 2.42 g/cm^3. Finally, having in mind that the densities of AlPO-18 and for the mixture (Al_2O_3 : P_2O_5) are 2.42 g/cm^3 and 3.00 g/cm^3, respectively it was predicted that 1g of each substance, either the AlPO-18 or the bulk Al_2O_3 : P_2O_5 mixture occupied 0.41 cm^3 and 0.33 cm^3. Therefore the difference between these two values is used to calculate the pore volume of AlPO-18, which is 0.08 cm^3/g.

Having in mind the difference between the specific pore volume calculated from the refractive index modelling, 0.08 cm^3/g, and that obtained from the N_2-sorption measurements, 0.7cm^3/g, we conclude that AlPO-18 pores do not remain empty after the particles are incorporated in the photopolymer. Since the size of the pores is relatively small (3.8 Å) and none of the organic components of the photopolymer are small enough to penetrate the openings, we can assume that the openings are filled with the water used as a solvent for the photopolymer.

This assumption is also consistent with the fact that the AlPO-18 particles are extremely hydrophilic.[38]

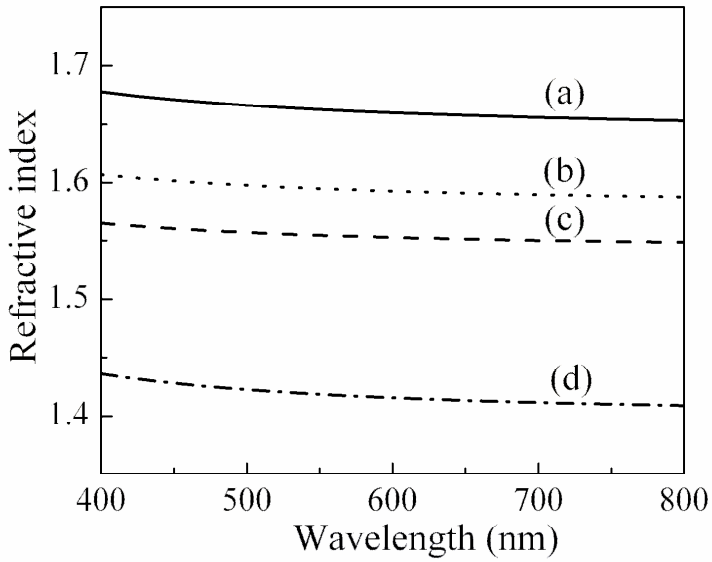

Figure 8. Dispersion curves of refractive index for (a) Al_2O_3, (b) mixture of Al_2O_3: P_2O_5 = 1:1 (c) P_2O_5, and (d) AlPO-18

The optical properties of the pure photopolymer layers and those doped with AlPO-18 nanoparticles were further characterized, by measuring their absorption. The absorption coefficients of the layers with different thicknesses are determined by UV-Vis spectroscopy using the Beer-Lambert law. The absorption coefficients for undoped and doped with 10 wt. % AlPO-18 nanoparticles layers are 79 ± 3 cm^{-1} and 84 ± 3 cm^{-1} at wavelength of 532 nm. The similar values indicate insignificant optical losses due to the incorporation of AlPO-18 nanoparticles into the photopolymer. The good optical quality of the layers was confirmed by diffuse reflectance measurements showing that even for heavily doped photopolymer (10 wt. % AlPO-18) the scattered intensity is less than 1 %.

Surface characterization of photopolymer layers doped with AlPO-18 nanocrystals. In addition to the bulk characterization of the photopolymer layers doped with AlPO-18 crystals, the surface properties were studied using a White Light Interferometric Surface profiler. Figure 9 presents the surface of photopolymer layers with different concentrations of AlPO-18 particles.

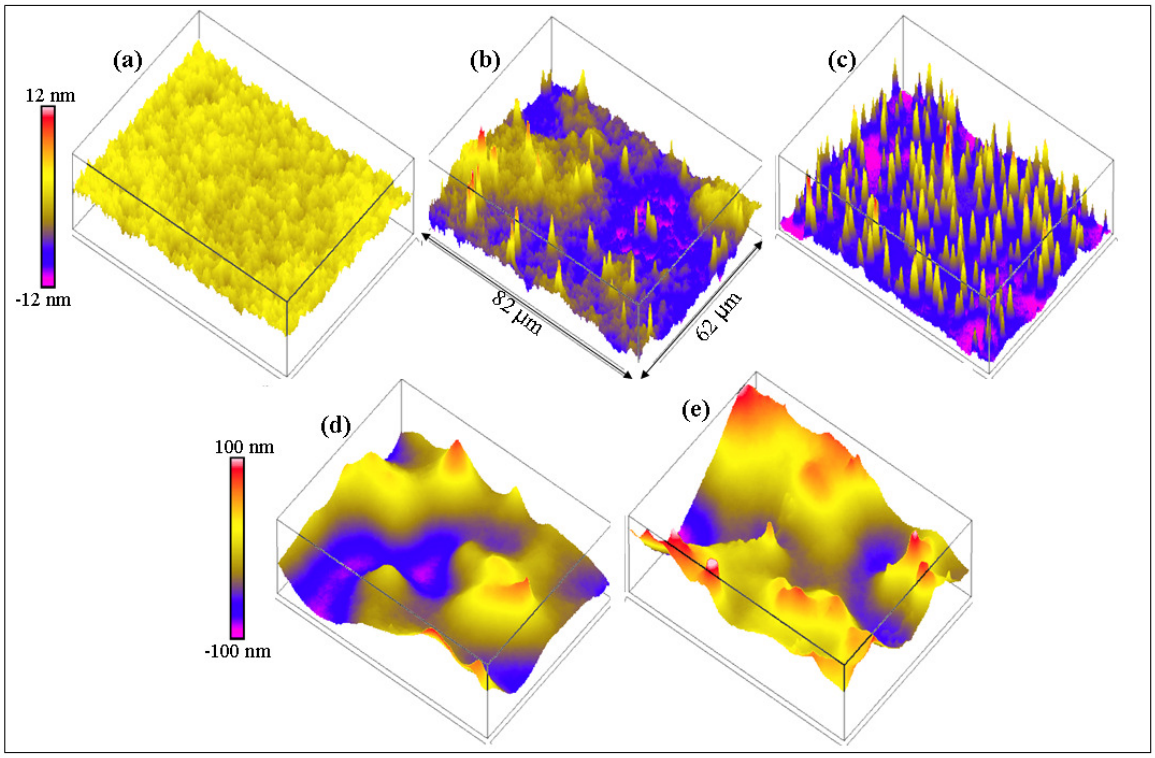

Figure 9. Surface profiles of photopolymer layers doped with (a) 0, (b) 2.5, (c) 3.5, (d) 5 and (e) 10 wt. % AlPO-18 nanoparticles measured using a White Light Interferometric Surface profiler.

As can be seen the surface roughness of the initially flat undoped layer increases with the increasing concentration of the AlPO-18 nanoparticles. The change of the surface roughness is due to the formation of aggregates from the AlPO-18 nanocrystals predominantly situated on the top of the layers. The roughness of the layers increases from 0.8 nm to 3.0 nm to 32 nm to 37 nm for undoped, 2.5 wt. %, 5 wt. % and 10 wt. % doped layers, respectively. Due to the low optical contrast between the AlPO-18 nanoparticles and the photopolymer, the losses due to the scattering do not exceed 1 %.

Holographic recording in photopolymer layers doped with AlPO-18nanocrsytals. The holographic properties of undoped photopolymer layers and layers containing AlPO-18

nanoparticles were investigated for two spatial frequencies (500 and 2000 lmm^{-1}) using a constant recording intensity of 5 $mWcm^{-2}$ for an exposure time of 120 s (exposure energy 600 mJ/cm^2) (Figure 10). The concentration of AlPO-18 nanoparticles ranged from 0 wt. % to 10 wt. %.

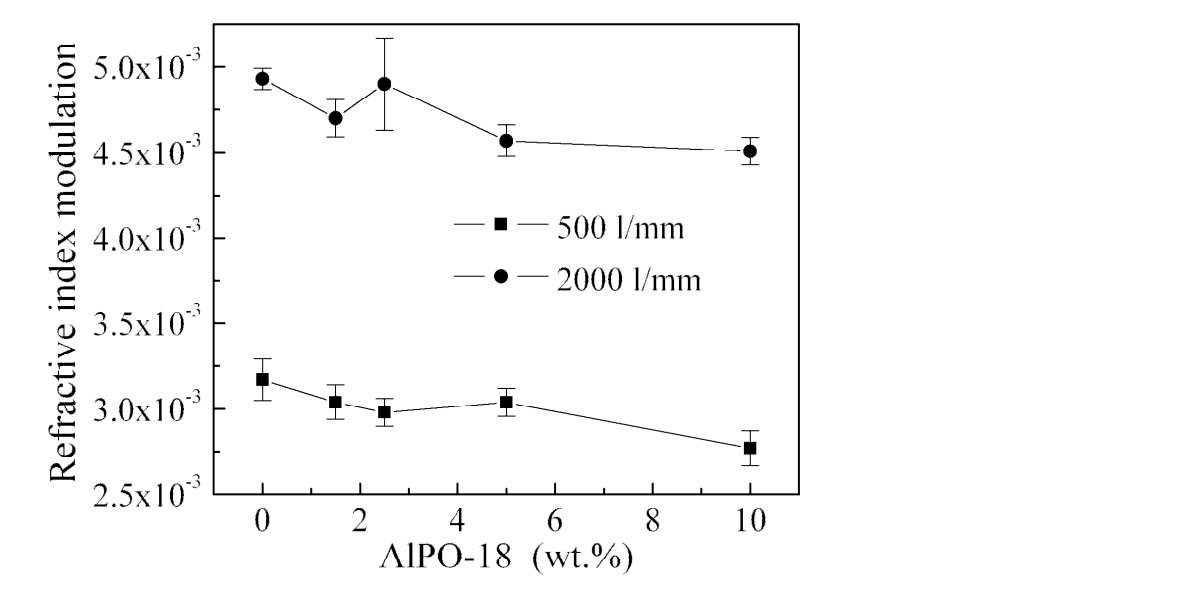

Figure 10. Holographic properties of photopolymer layers doped with AlPO-18 nanoparticles at spatial frequencies of 500 and 2000 l/mm (exposure of 600 mJ/cm^2).

As can be seen from Figure10, all photopolymer layers used in recording at 2000 l/mm spatial frequency show consistently higher refractive modulation then the layers recorded at 500 l/mm spatial frequency. Such dependence can be explained in the undoped layers because with the decrease in the grating period the distance traveled by the photopolymer components in order to achieve their redistribution decreases, which is resulting in greater refractive index modulation. One should also note that increased concentration of nanoparticles does not result in an increased refractive index modulation. Possible reasons for this are the absence of redistribution of nanoparticles or a very small amount of nanoparticles are redistributed or the difference between the nanoparticles refractive index and the photopolymer matrix is not enough to increase the refractive index modulation. From Figures 7 and 8 one can estimate the refractive index of nanoparticles filled with H_2O to be 1.414 at 633 nm, and the refractive index of the undoped photopolymer matrix at this wavelength is 1.499, i.e. a difference of 0.085 is measured. The next

step was to see if there is a redistribution of the nanoparticles as a result of the holographic recording in the layers.

Confocal Raman spectroscopy was used to study the light induced redistribution of AlPO-18 nanoparticles during the holographic recording. The spectra of pure photopolymer, pure AlPO-18 and photopolymer doped with 10 wt. % AlPO-18 nanoparticles are shown in Figure 11. Well resolved peaks at 421 cm^{-1} originating from T-O-T vibrations of the AEI framework type structure can be seen in both pure AlPO-18 and photopolymer doped with AlPO-18 nanocrystals (Figure 11).

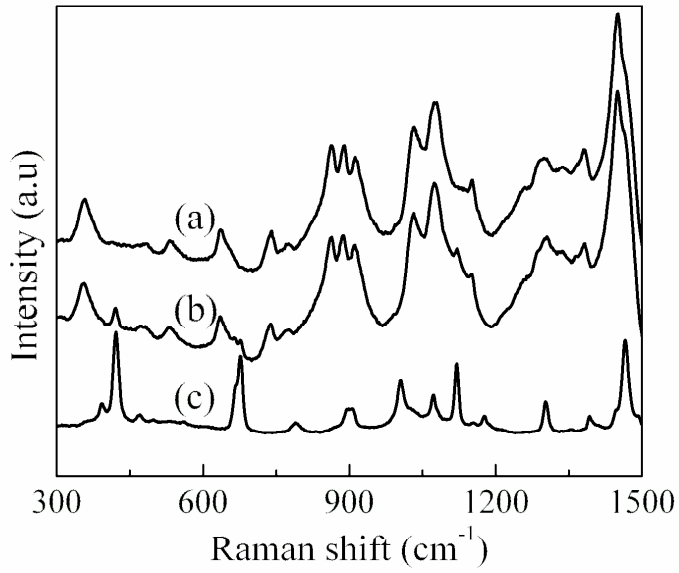

Figure 11. Raman spectra of (a) acrylamide-based photopolymer; (b) acrylamide-based photopolymer doped with AlPO-18 nanoparticles (10 wt. %) and (c) pure AlPO-18

The intensity of the Raman peak at 421 cm^{-1} depends on the concentration of AlPO-18 in the layers. To study the light induced redistribution of AlPO-18 nanoparticle, transmission gratings with a spatial frequency of 200 l/mm (period of 5 μm) were recorded in the layers with 1, 2.5 and 7.5 wt. % AlPO-18 at recording intensities of 1, 5 and 10 mW/cm^2. The Raman peak intensity at 421 cm^{-1} was monitored in the direction of the grating vector in steps of 1 μm and compared with the distribution of the Raman peak intensity of AlPO-18 outside the grating (Figure 12).

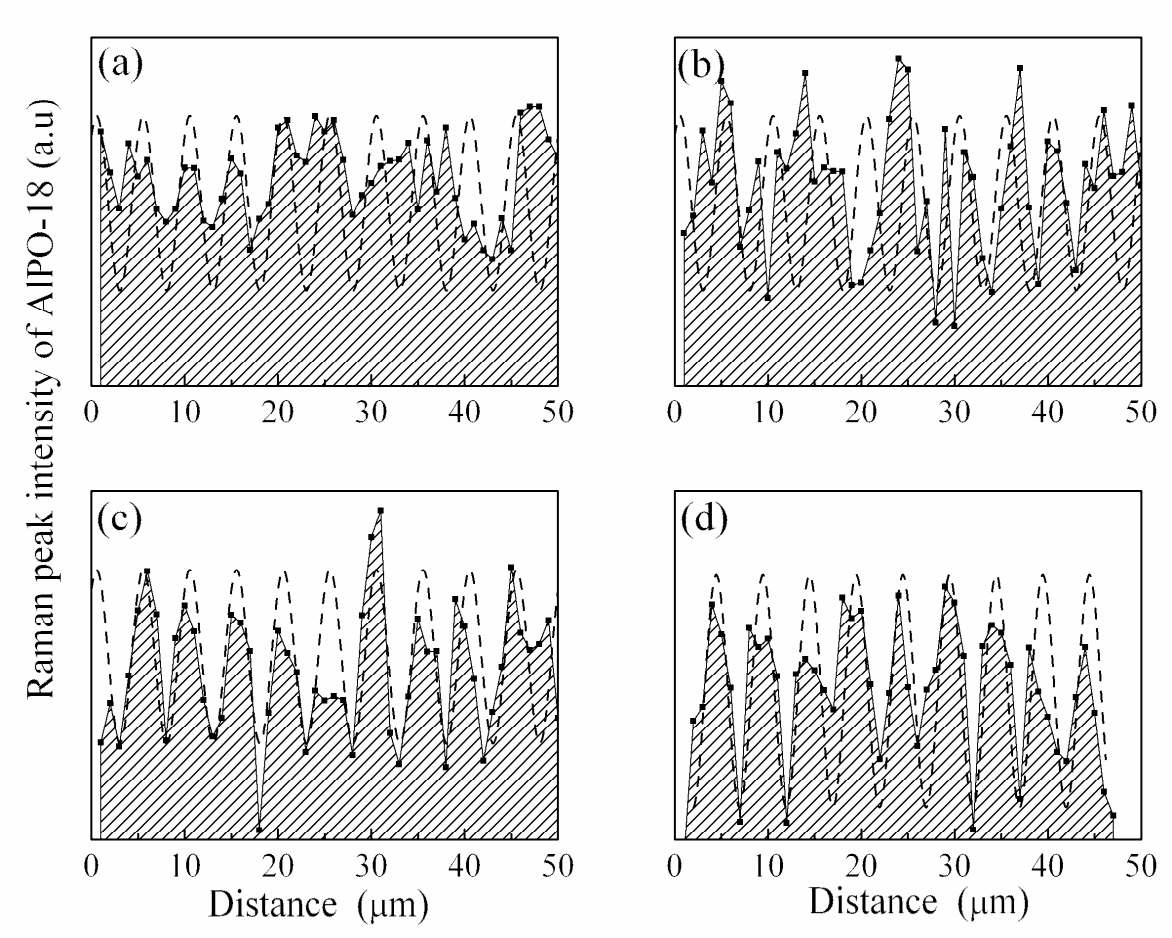

Figure 12. Raman peak intensity (421 cm^{-1}) corresponding to AlPO-18 for photopolymer layers doped with 2.5 wt. % nanocrystals: (a, b) outside the grating and (c, d) inside the grating (in direction parallel to the grating vector) recorded with a period of 5 μm with intensity of 10 $mWcm^{-2}$. The dotted line presents a sine function with a period of 5 μm

As can be seen from Figure 12, the variation of the intensity of the Raman peak at 421 cm^{-1} outside the grating is random. In the direction of the grating vector, a spatially periodic distribution of the intensity of the Raman signal is observed with a period of 5 μm, which is in a good agreement with the known period of the grating. The greatest variation in the intensity of the Raman peak was observed in the gratings recorded with intensity of 10 mW/cm^2 in layers

doped with 2.5 wt% AlPO-18 nanoparticles. If one assumes that the Raman peak intensity is linearly proportional to the concentration of the nanoparticles, then the redistributed fraction of the nanoparticles is 31 % from the total volume. Using equation (3) the refractive index modulation contribution from the redistribution of the nanoparticles can be calculated.

Since the density of the water filled nanoparticles is 2.42g/cm^3, and knowing the weight of the nanoparticles present in a single nanocomposite layer, one can calculate that the volume fraction of the nanoparticles in the layer is 0.75 %, thus the volume fraction of the redistributed nanoparticles is calculated to be 2.3×10^{-3}. The difference between the refractive index of the host photopolymer and water filled nanoparticles is estimated to be 0.085. Thus the expected refractive index modulation contributed by the redistributed nanoparticles is calculated to be 1.3×10^{-4}. This result explains why there was no improvement of the refractive index modulation through holographic recording in the layers doped with AlPO-18 in comparison to the undoped layers. The picture will change if by some means the water in the pores of the nanoparticles is expelled. The difference in the refractive index between the host polymer matrix (1.499) and the refractive index of the empty nanoparticles (1.239) is approximately three times greater, about 0.26. In the following experiment this effect is demonstrated to be useful for the design of irreversible humidity sensors. It is shown that the diffraction efficiency of initially baked layers (with empty pores) undergoes irreversible change when the sensor is exposed to high humidity (and the microporous nanoparticles absorb water).

Volume transmission gratings for humidity sensing. Volume transmission gratings recorded in photopolymer and in photopolymer doped with 2.5 wt. %, of AlPO-18 nanoparticles were tested as irreversible humidity holographic sensors. Irreversible response of the holograms in a humidity controlled environment by monitoring the evolution of the diffraction efficiency is measured. Initially, after recording, the layers were exposed to high temperature, 120 ºC, in order to expel the water from the nanoparticles' pores. Then the diffraction efficiency of the layers was measured at a relative humidity (RH) of 15 %. Further, the layers were exposed to high humidity of 60 %. The evolution of the diffraction efficiency was monitored after the humidity in the chamber was restored to the initial value of 15 % (Figure 13). The diffraction efficiency of the undoped layer reaches its initial value (Figure13b), while the diffraction efficiency in the doped layers never returns to the initial value (Figure 13a). If one repeats the calculations in section *4.3,* this time for the empty pores of AlPO-18, one can estimate that the refractive index contribution

of the redistributed nanoparticles is $3.9x10^{-4}$. Since the initial diffraction efficiency (after baking) of the doped layer was 70 %, the corresponding refractive index modulation at the start of the experiment using equation 4 can be estimated. After exposure to high humidity this refractive index modulation will decrease by $2.6x10^{-4}$ (the difference between the contribution of the redistributed nanoparticles with empty and the full pores with water). Thus the final diffraction efficiency of the hologram was estimated to be 63.4 %. The measured diffraction efficiency is 64 %, which is in a very good agreement with the value determined from the theoretical model. Although this is a relatively small irreversible change in the diffraction efficiency of the hologram, it is achieved by adding a modest volume of AlPO-18 nanoparticles (less than 1%). Therefore we believe that these results reveal the potential of the proposed approach for future design of holographic sensors.

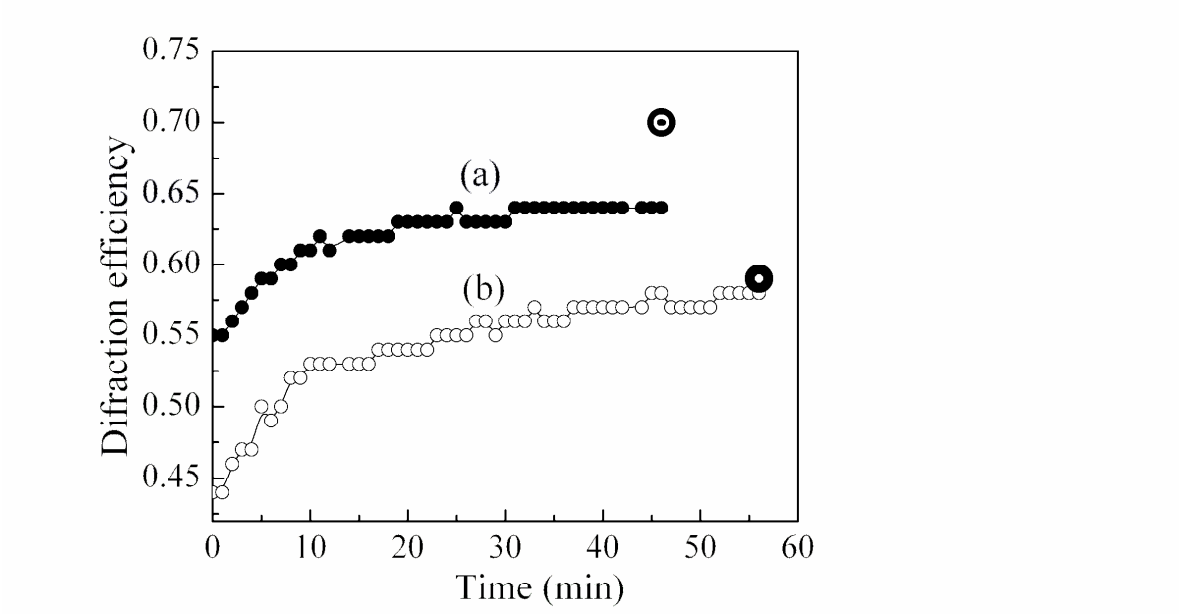

Figure 13. Diffraction efficiency evolution over time (from RH 60 % to 15 %), a) photopolymer doped with AlPO-18 2.5 wt.% b) undoped photopolymer, bold circles denote initial diffraction efficiency values, measured before exposure to high humidity (15 % RH). In the case of photopolymer, it takes around 1 hour to reach the initial value of diffraction efficiency (measured at 15 % RH). With the addition of AlPO-18 nanoparticles, a plateau is observed with a value below the initial diffraction efficiency, thus indicating an irreversible sensing properties.

Conclusions

The changes in volume and surface properties of the photopolymer layers doped with microporous aluminophosphate nanoparticles (AlPO-18) are investigated. Volume transmission gratings at different spatial frequencies were recorded, and show that a light induced redistribution of the particles occurs during the holographic recording. Optimal conditions for this effect include a concentration of the AlPO-18 nanocrystals of 2.5 wt. % and a recording intensity of 10 $mWcm^{-2}$.

The optical properties of the photopolymer layers combined with the capability of light-induced redistribution of the AlPO-18 nanoparticles during the holographic recording are very important parameters, which are explored for fabrication of holographic humidity indicator. The addition of AlPO-18 to the layer introduced an irreversible change in the diffraction efficiency of the holographic gratings in the layers under exposure to high humidity. This would be important for situations where regardless of current (potentially lower) humidity levels, the possible higher levels of humidity were earlier prevalent could be estimated.

Acknowledgements: The authors (SM, EPN) gratefully acknowledged funding from the SRIF PNANO-ANR Project. IRCSET is acknowledged for its support through the Ulysses travel Programme. This work was supported by the Technological Sector Research: Strand I - Post-Graduate R&D Skills Programme. The authors acknowledge the FOCAS institute and the SARA Programme at Dublin Institute of Technology for technical and financial support. TB would like to thank to COST Action MP0604 for the STSM at IEO, Dublin Institute of Technology.

References

(1) Guntaka, S.; Toal, V.; Martin, S. *Appl. Opt.* **2002***, 41,* 7475.

(2) Trout, T.J.; Schmieg, J.J.; Gambogi, W.J.; Weber, A.M. *Adv. Mater.* **1998**, *10,* 1219.

(3) Marshall, A.J.; Blyth, J.; Davidson, C.; Lowe, C.R. *Anal. Chem.* **2003,** *75*, 4423.

(4) Sherif, H.; Naydenova, I.; Martin, S.; McGinn, C.; Toal, V. *J. Opt. A, Pure Appl. Opt.* **2005**, 7, 255.

(5) http://www.aprilisinc.com/.

(6) http://www.inphase-technologies.com/.

(7) Lhadi, M. "*Hybrid Nanocomposites for Nanotechnology: Electronic, Optical, Magnetic and Biomedical Applications"*, Springer, New York, **2009**.

(8) Gomez-Romero, P. *Adv. Mater*. **2001**, *13*, 163.

(9) Günes, S.; Neugebauer, H., Sariciftci, N. *Chem. Rev.* **2007**, *107*, 1324

(10) Sanchez, C.; Julian, B.; Belleville, P.; Popall, M. J. *Mater. Chem.* **2005**, *1*5, 3559.

(11) Guha, S.; Haight, R. A.; Bojarczuk, N. A.; Kisker, D. W. *J. Appl. Phys.* **1997**, *82*, 4126.

(12) Naydenova, I.; Toal, V. "Nanoparticle Doped Photopolymers for Holographic Applications" in Ordered Porous Solids: Recent Advances and Prospects (Eds. V. Valtchev, S. Mintova and M. Tsapatsis) **2008**.

(13) Suzuki, N.; Tomita, Y. *Appl. Opt.* **2004,** *43*, 2125.

(14) Tomita, Y.; Chikama, K.; Nohara, Y.; Suzuki, N.; Furushima, K.; Endoh, Y. *Opt. Letters* **2006,** *31,* 1402.

(15) Suzuki, N.; Tomita, Y.; Kojima, T. *Appl. Phys. Lett*. **2002,** *81***,** 4121.

(16) Smirnova, T.; Sakhno, O.; Bezrodnyj, V.; Stumpe, J. *Appl. Physics* **2005**, *B80*, 947.

(17) Suzuki, N.; Tomita,Y.; Ohmori, K.; Hidaka, M.; Chikama, K. *Opt. Express* **2006,** *14*, 12712.

(18) Tomita, Y.; Nishibiraki, H., *Appl*. *Phys. Lett.* **2003,** 83, 410.

(19) Sanchez, C.; Escuti, M.; Heesh, C.; Bastiaansen, C.; Broer, D.; Loos, J.; Nussbaumer, R. *Adv. Funct. Mat.* **2005,** 15 1623.

(20) Omura, K.; Tomita, Y., *Appl. Phys.* **2010**, 107, 023107.

(21) Naydenova, I.; Sherif, H.; Mintova, S.; Martin, S.; Toal, V. *Proc. SPIE* **2006,** 6252.

(22) Leite, E.; Naydenova, I.; Pandey, N.; Babeva, T.; Majano, G.; Mintova, S.; Toal, V. *J. Opt. A: Pure Appl. Opt.* **2009,** *11*, 024016.

(23) Babeva, T.; Todorov, R.; Mintova, S.; Yovcheva, T.; Naydenova, I.; Toal, V. *J. Opt. A: Pure Appl. Opt.* **2009**, 11 024015.

(24) Mintova, S.; Valtchev, V.; Onfroy, T.; Marichal, C.; Knozinger, H.; Bein, T. *Microporous Mesoporous Mater.* **2006,** *90,* 237.

(25) Larlus, O.; Mintova, S.; Valtchev, V.; Jean, B.; Metzger, T.H.; Bein, T.; *Appl. Surface Sci*. **2004**, *226*, 155.

(26) Ng, E.-P.; Mintova, S. *Microporous Mesoporous Mater.* **2008,** *114*, 1.

(27) Baerlocher, Ch.; McCusker, L.B.; Olson, D.H. *Atlas of Zeolite Framework Types*, 6th revised edition, Elsevier, Amsterdam, **2007.**

(28) Kogelnik, H.; "Coupled-wave theory for thick hologram gratings" *Bell. Syst. Tech. J*. **1969,** *48,* 2909.

(29) Vaia R., Dennis C., Natarajan L., Tondiglia V., Tomlin D., Bunning T. *Adv. Mat.* **2001**, 13 1570.

(30) Martin, S.; Leclere, P.; Renotte, Y.; Toal V.; Lion, Y. *Opt. Eng.* **1994,** *33*, 3942.

(31) Hiemanz, P. C.; Rajagopalan, R. "Principles of colloid and surface chemistry", Marcel Dekker Inc, New York-Basel-Hong Kong, **1997**.

(32) IUPAC Recommendation *Pure Appl. Chem.* **1994**, *66*, 1739.

(33) Reinecke, H.; Spells, J.; Sacristán, J.; Yarwood, J.; Mijangos, C. *Appl. Spectroscopy* **2001**, 55, 1660.

(34) Yovcheva, T.;Babeva, Tz.; Nikolova, K.; Mekishev, G. *J. Opt. A: Pure Appl. Opt*. **2008**, *10*, 055008.

(35) Palik, Edward D. "Handbook of Optical Constants of Solids" Elsevier, Amsterdam, **1998.** pp: 766.

(36) Katsuyama, T.; Suganuma, T.;Ishida, K.; Toda, G. *Optics Comm.* **1977**, *21*, 182.

(37) "Handbook of Chemistry and Physics", 66th Edition, Eds. R.C. Weast, M.J. Astle, W.H. Beyer, CRC Press, Inc. Boca Raton, Florida, 1985.

(38) Ng, E.-P.; Delmotte, L.; Mintova, S. *ChemSusChem* **2009**, *2*, 255.

(39) Sakhno O., Goldenberg L., Stumpe J., Smirnova T., *Nanotechnology* 18 **2007**, 105704.

(40) Sanchez, C.; Escuti, M.; Heesh, C.; Bastiaansen, C.; Broer, D.; Loos, J.; Nussbaumer, R. *Adv. Funct. Mat.* **2005,** *15* 1623.

Table 1 Properties of nanosized AlPO-18 samples.

Samples	**Al/P ratio**	**Surface area** (cm^2/g)	**Pore volume** (cm^3/g)	**Micropore volume** (cm^3/g)	**Zeta potential**[a] (mV)	**Crystal size range** (nm)
Sample 1	1.02	580	0.71	0.21 cm^3/g	-47	150-220
Sample 2	1.03	512	0.72	0.20 cm^3/g	-41	180-250

[a]Measurements are performed in water solution with a constant concentration of 6 wt.% at pH=7 and 25 °C.

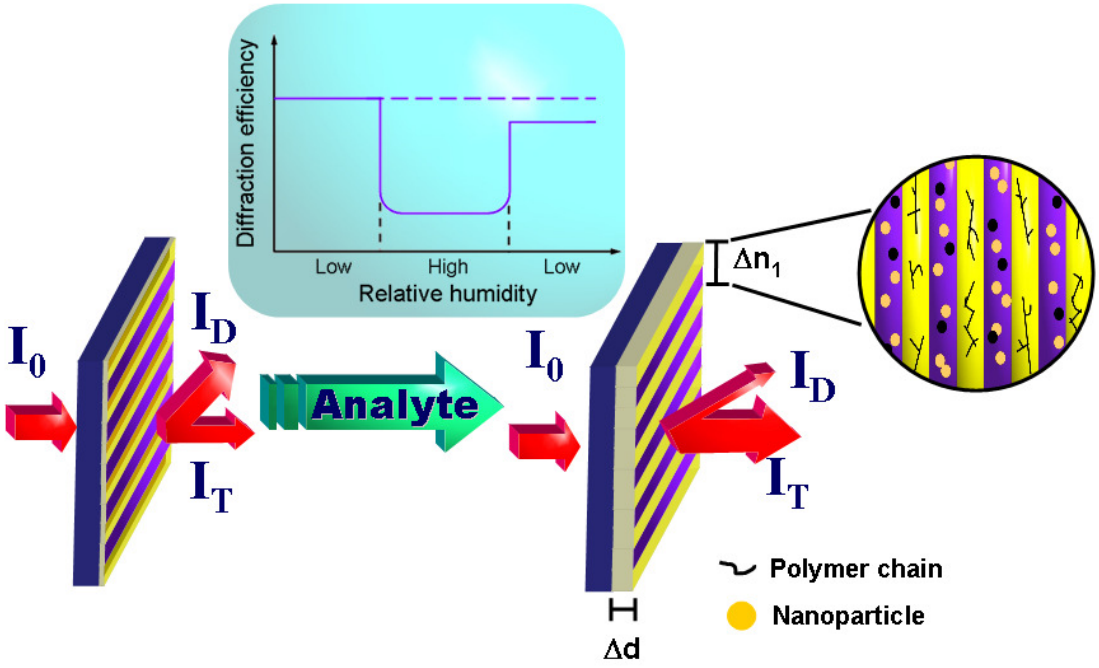
Diffraction efficiency
Low
High
Low
Relative humidity
I_0
I_D
I_T
Analyte
I_0
I_D
I_T
Δn_1
Δd
Polymer chain
Nanoparticle